

An x-ray setup to investigate the atomic order of confined liquids in slit geometry

M. Lippmann, A. Ehnes, and O. H. Seeck

Citation: [Review of Scientific Instruments](#) **85**, 015106 (2014); doi: 10.1063/1.4860057

View online: <http://dx.doi.org/10.1063/1.4860057>

View Table of Contents: <http://scitation.aip.org/content/aip/journal/rsi/85/1?ver=pdfcov>

Published by the [AIP Publishing](#)



Re-register for Table of Content Alerts

Create a profile.



Sign up today!



An x-ray setup to investigate the atomic order of confined liquids in slit geometry

M. Lippmann, A. Ehnes, and O. H. Seeck

Deutsches Elektronen-Synchrotron DESY, Notkestr. 85, 22607 Hamburg, Germany

(Received 18 October 2013; accepted 16 December 2013; published online 13 January 2014)

A setup has been designed to investigate thin films of confined liquids with the use of X-ray scattering methods. The confinement is realized between the flat culets of a pair of diamonds by positioning and orienting the lower diamond with nanometer and micro radian accuracy. We routinely achieve gaps between 5 and 50 nm at culet diameters of 200 μm . With this setup and a micro focused X-ray beam we have investigated the in-plane and the out-of-plane atomic order of benzene with atomic resolution. © 2014 AIP Publishing LLC. [<http://dx.doi.org/10.1063/1.4860057>]

I. INTRODUCTION

The properties of bulk matter and matter in a confined state differ significantly. Confinement means that at least one dimension of the sample is smaller than a few molecular diameters. It can be realized as pores (confinement in 3 dimensions),¹ capillaries (2 dimensions),² or slits (confinement in one dimension)^{3–7} and each of the realizations has very interesting implications on the nature of the matter. In general, the confinement strongly influences the mobility of the molecules. In the case of soft matter parameters such as the glass transition, the melting temperature, and the shear response are affected. Also due to the broken symmetry in the direction of the confinement, the atomic order of liquids is altered.

In the following, we restrict ourselves to confinement in slit geometry. First experiments to investigate soft matter in this geometry have been conducted by the group of Israelachvili^{3,8} using a Surface Force Apparatus (SFA). The SFA exhibits crossed cylinders as gap-defining device to confine a liquid film at an area of about $200 \times 200 \mu\text{m}^2$. It was used to measure the mechanical properties of the film and proved molecular layering normal to the confined surfaces at gap sizes less than ten times the molecular diameter.⁴ Later, the groups of Granick⁹ and van der Veen¹⁰ constructed environments which are dedicated to X-ray diffraction methods. X-ray diffraction is the only direct tool to determine the structure of a confined liquid on atomic length scales. So-called out-of-plane measurements such as X-ray reflectivity are sensitive to molecular layering perpendicular to the surface whereas in-plane measurements can resolve ordering effects along the confinement areas. The design of such setups is challenging. First, the gap between the two confining surfaces must be accurately defined in terms of the gap size. Second, the confinement area must be accessible for the incident and diffracted X-rays in a relatively large solid angle.

One of the first successful designs of a confined liquid X-ray cell was accomplished by the group of van der Veen (see Zwanenburg *et al.*¹⁰). They were able to confine colloids to gaps of micrometer size. Smaller gaps down to nanometer range have been achieved later by Seeck *et al.*,⁵ Becker,¹¹ and Perret *et al.*¹² Becker has investigated the smectic phase

of 8CB liquid crystals using an SFA, where the X-ray beam transmits perpendicular through the curved mica substrates (see SFA as mentioned above) and the confined layer. However, the scattered signal from films thinner than 8 nm was very weak and buried under the scattering background from the substrates. Seeck *et al.* used polished flat single crystal silicon substrates with an area of several mm^2 and Octamethylcyclotetrasiloxane (OMCTS) as a liquid. The X-rays illuminated the confined liquid from the side. In this geometry the scattered signal was strong, and the silicon substrates were virtually background-less. However, it was extremely challenging to prepare the surfaces and the risk of failure was significant. The cell of Perret is based on the crossed cylinder design of a SFA, again using mica, but accessible from the side. She was able to confine the non-polar liquid Tetrakis(Trimethylsiloxy)Silane (TTMSS) down to gap sizes of 10 nm.

Basically all X-ray experiments up to now have been done in forward scattering, so they are of the type reflectivity or small angle scattering with lacking atomic resolution along the surfaces. We are aiming for measurements of the atomic order in the out-of-plane direction additionally to the in-plane direction. For this we have designed a new setup which is presented in the following.

II. GENERAL DESIGN CONSIDERATIONS

For the realization of a setup to measure confined liquids as described above three types of constraints arise:

- (1) Constraints regarding the geometry: The setup must allow for nanometer sized gaps with an error of less than a few 0.1 nm. The parallelism must be better than a few 0.1 nm deviation over the illuminated area. For the roughness of the confining substrates the same holds. Settled dust on the surfaces is unacceptable. Also, the substrates have to withstand pressure and chemicals. The whole setup must fit into an X-ray diffractometer, in our case the Kohzu NZD-3 at the high resolution diffraction beamline P08 at the third generation synchrotron radiation source PETRA III at DESY in Hamburg.¹³

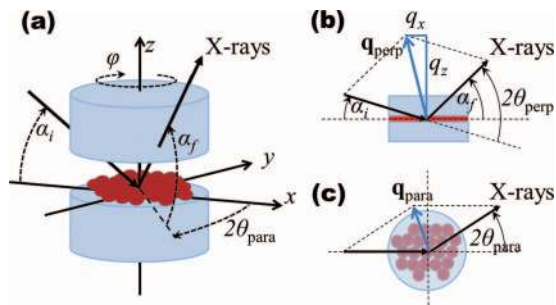


FIG. 1. The geometry of an X-ray experiment at confined liquids in slit geometry. (a) The two substrates are shown with the liquid atoms as spheres, the incident and outgoing X-ray beams and all relevant angles. (b) Projections from the side and (c) projection from the top. The out-of-plane wave vector transfer q_{perp} and the in-plane wave vector transfer q_{para} are displayed.

- (2) Constraints regarding the liquid handling: The liquid must not be injected directly into the gap to avoid contamination with small particles. It has rather to be evaporated from the bottom part of the cell and deposited from vapor onto the substrates. During the experiment external parameters such as temperature and vapor pressure have to be constant. To watch the liquid in the gap by means of optical methods one microscope from the top and one from the side are required.
- (3) Constraints regarding X-ray scattering: The substrates have to be virtually transparent to X-ray beams to keep absorption effects and scattering background low. The arrangement of the substrates must allow for wave vector transfers \mathbf{q} (see, e.g., the book of Als-Nielsen¹⁴ for the definition of \mathbf{q}), along and vertical to the substrate normal, such that they are sufficiently large for atomic resolution. This usually means $|\mathbf{q}| > 3 \text{ \AA}^{-1}$ for liquids with molecules larger than 4 Å. Furthermore, a rotation around the substrate normal, the azimuth φ , must be available for detection of possible 2D crystal arrangements of the molecules (see Fig. 1).

From the first list of constraints follows that the substrates should be extremely well polished and prepared under cleanroom conditions. Also, at least one of the substrates has to be positioned and oriented, e.g., by piezo actuators to assure the required accuracy. Furthermore, the confining surfaces should be small for easy cleaning and aligning. However, small surface also means that high pressure can arise on closing the gap. Therefore, the substrates must withstand mechanical stress. Adequate materials are diamond, sapphire, and other similar materials.

As for the second list of constraints the confining substrates should be located inside a hermetic cell which has to be assembled in a clean room. The liquid must be injectable into a reservoir at the bottom of the cell. From there it is evaporated by heaters for deposition into the gap which has to be macroscopically large (some 10 μm) for this procedure. Consequently, the gap movement should not only be accurate on the nanometer range but furthermore the maximum opening should be some 10 μm .

The last point implies that the substrates should be made of low Z materials where Z is the atomic number. They should

be perfect crystals with small unit cell to avoid background scattering at low \mathbf{q} . The setup should be more or less axially symmetric to allow for azimuthal rotations. Therefore, the substrates should be small pieces with cylindrical symmetry and made from sapphire, quartz, or diamond. Crossed cylinders covered with mica which are standard for SFAs are not suitable. Finally, the cell needs to exhibit large X-ray windows also from low Z materials and with low scattering background.

Complying with the three points, we have designed a setup which is based on a diamond anvil cell.¹⁵ The substrates are single crystal diamonds. The confining area is formed by two small culets with diameter 200 μm . The upper diamond can roughly be aligned by manual mechanics. The lower diamond is motorized and additionally tunable by a 3 axes piezo actuator. The diamonds are concealed inside a hermetic cell which enables out-of-plane X-ray reflectivity measurements up to $q_{\text{perp}} = 3 \text{ \AA}^{-1}$ and in-plane diffraction up to $q_{\text{para}} = 7 \text{ \AA}^{-1}$ at a photon energy of 18 keV. The X-ray windows are made from 20 μm thick aluminum foils which exhibit low scattering background (for details see below). Two optical microscopes are mounted at the diffractometer from the top and from the side to inspect the gap. The whole setup can be cleaned, loaded, and assembled in a local cleanroom facility or laminar flow box and then transferred to the beamline. The liquid can be injected into the cell at the beamline using a syringe.

III. TECHNICAL DESIGN, ALIGNMENT PROCEDURES, AND CONDUCTING THE EXPERIMENT

The substrates in use are single crystal diamonds (Almax Industries). As mention above the culet diameter is 200 μm (see Figs. 2(a) and 2(b)). Best results have been achieved with culet surfaces oriented along the crystallographic 100 planes. The quality of the diamond surfaces has been observed with Atom Force Microscope (AFM) (see Fig. 2(e)) and confirmed by means of X-ray reflectivity measurement. The AFM map shows that the surface has a stripe structure with groves of about 1.4 nm depth. The root mean square (rms) roughness obtained from the reflectivity scans is around 0.7 nm and in agreement with the AFM results.

Both diamonds are clamped to cylindrical holders with through holes for the optical microscope looking from the top and the respective light source from the bottom. At closed gaps, the maximum vertical opening angle for the X-ray beam is $\pm 10^\circ$ (see Fig. 3). The diamond holders are fixed to individual stands between which the hermetic casing is installed. This assembly is called confined liquid cell in the following (see Fig. 4). The casing has X-ray windows along the beam (with a $\pm 55^\circ$ horizontal opening) and glass windows for the microscopes. The X-ray windows are made from 20 μm thick aluminum foils. Aluminum has a higher X-ray absorption compared to low absorbing Kapton[®] or Mylar[®] organic plastic foils. However, the X-ray scattering background of organic materials is highest at the position where the scattering signal of the confined liquids is expected to appear. In contrast, the background of aluminum is mostly concentrated at the powder diffraction rings which are offset from the scattering

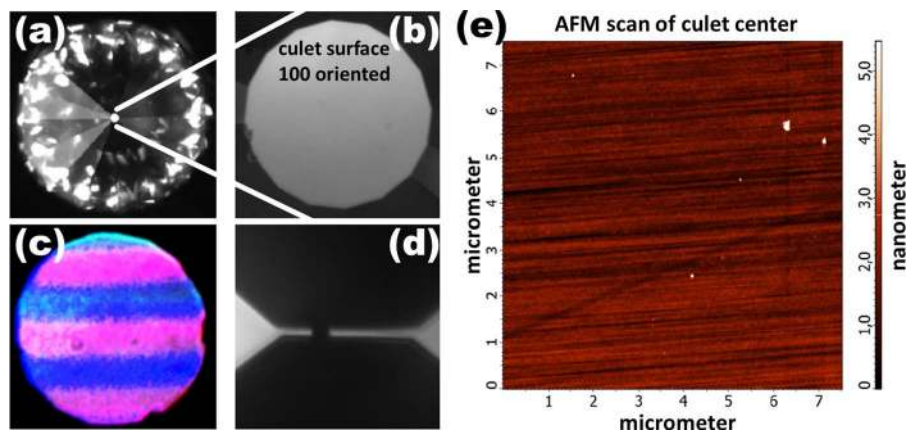


FIG. 2. (a) One of the diamonds looking onto the culet. (b) The culet with 200 μm diameter, magnified. (c) Optical fringes at a misaligned gap of approximately 1 μm size, looking from top. (d) Side view of the gap with a small droplet of OMCTS. The gap size is approximately 15 μm . (e) An AFM image from the center part of the culet. The scratches are approximately 1.4 nm deep.

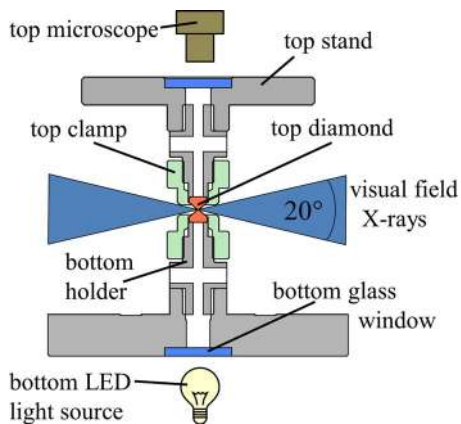


FIG. 3. A cut through the confined liquid cell containing the gap forming diamonds. The diamonds are fixed to the holders which are mounted to the stands. The stands and the holders are hollow to allow for optical microscopy.

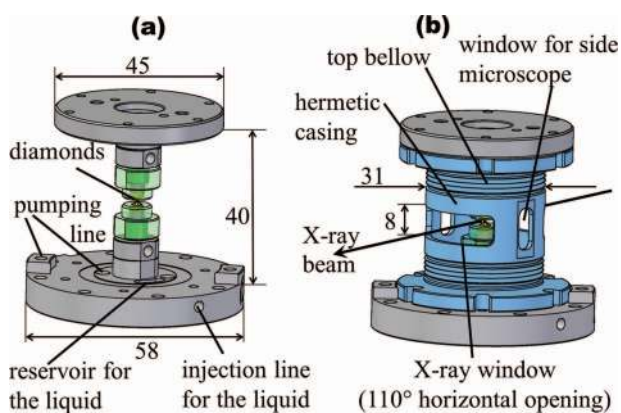


FIG. 4. The confined liquid cell containing the diamonds and showing some dimensions in millimeters. (a) Naked view from Fig. 3 depicting the lines to inject the liquid and to pump (not used here). (b) With installed casing (uncovered windows).

of the liquids. This makes aluminum superior over organic foils.

Two small bellows from the top and the bottom of the casing allow tilting and translating of the diamonds with respect to each other and thus enable precise alignment of the gap. For the alignment procedure the microscopes from the top and the side are essential. To align the culet surfaces exactly parallel the optical interference pattern which can be seen from the top is inspected (see Fig. 2(c)). It vanishes on correct alignment. Gap sizes larger than a few μm can easily be monitored by the side microscope.

To align the culet surfaces and to define the gap size a set of coarse and fine movements exist. For this, the confined liquid cell is mounted between the aligning setup (see Fig. 5). The top diamond surface can be coarsely aligned along z (10 mm travel with accuracy 1 μm) and oriented in the

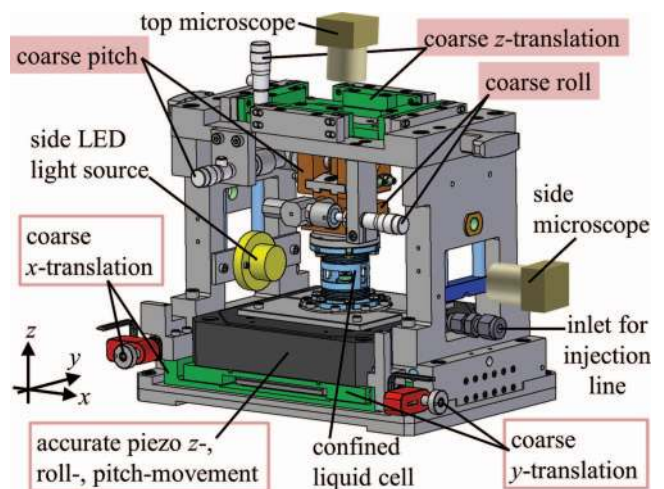


FIG. 5. The setup for measurements at confined liquids. The confined liquid cell is positioned in the center of the aligning setup. All labels which are highlighted point to movements of the top diamond. All labels which are framed point to movements of the bottom diamond.

pitch and roll ($\pm 2^\circ$ and 0.002° accuracy). The lower diamond is motorized with x - and y -translations (± 5 mm with step size of 30 nm). The translations have a very small step size but the position of the diamond is only controlled by microscopic observations with resolution of $1\ \mu\text{m}$. The fine alignment of the lower diamond is done by a triple axes piezo stage (Physik Instrumente PI P-528.TCD). It allows for $200\ \mu\text{m}$ travel with accuracy of 1 nm and ± 1 mrad tilting with a resolution of $0.1\ \mu\text{rad}$. The assembly of the setup and the pre-alignment are conducted in an ISO class 4 cleanroom.

It is very important to note that the alignment of the parallelism of the surfaces by means of optical microscopy is insufficient. The inspection of the interference pattern presented in Fig. 2(c) is only sensitive to distances larger than half of the wavelength of the visible light. Even assuming that a 10th of a wavelength would be detectable implies that the gap mismatch measured across the surface of the culets would be approximately 40 nm. At diameters of the culet of $200\ \mu\text{m}$ this offset corresponds to 0.01° . Complying with the constraints regarding the geometry which define a few 0.1 nm as tolerable gap mismatch this value is unacceptable.

Therefore, the fine alignment of the parallelism is done at the X-ray beamline. For this the position of the specular reflected signal of each culet is measured by tilting and rolling the surfaces and keeping the detector at fixed scattering angle (so-called rocking scan). The peak position of the reflection can be determined with an accuracy of 0.001° which corresponds to a gap mismatch of approximately 4 nm over the whole $200\ \mu\text{m}$ diameter. In fact, it turns out that for very small gaps and on pressure the parallelism tends to be even better as the whole setup is slightly elastic favoring parallel culet surfaces.

Gap sizes in the 1 or 2 nm range are not routinely achievable, yet. Already some small dust particles prevent very small gaps. However, applying pressure helps: On very small length scales the diamond can be elastically deformed.^{16,17} Therefore, if just a few nanoparticles are present on the surface they may on zero pressure prohibit small gaps but on pressure the average gap size may shrink. It seems even to be advantageous to have a few nanoparticles on the surface as they may be able to stabilize the gap against vibrations or collapsing due to forces such as generated by the Casimir effect.¹⁸

After assembly of the cell and pre-aligning the diamonds in the clean room the X-ray scattering experiments are carried out at a photon energy of 18 keV, which is perfectly suited for this experiments: The diamonds and the Al-windows are sufficiently transparent and the reciprocal space spans $\mathbf{q}_{\text{perp}} = \pm 3^\circ\ \text{\AA}^{-1}$ and $\mathbf{q}_{\text{para}} = \pm 7^\circ\ \text{\AA}^{-1}$. Furthermore, at this photon energy the scattering cross section of the organic molecules is still sufficiently high (which it is not at, e.g., 25 keV).

At the beamline and using the microscopes the confining gap is first centered to the pivot point of the diffractometer. Thereafter, the surfaces of the culets are characterized by means of X-ray reflectivity and grazing incidence diffraction.¹⁴ For this the gap is open at approximately $30\ \mu\text{m}$. Simultaneously, the parallelism of the surfaces has been aligned as described above. On success we inject a small

amount of the liquid ($\sim 200\ \mu\text{l}$) through the injection line, which is covered by a hermetic septum, into the reservoir inside the cell (see Fig. 5). By a careful heating procedure the liquid evaporates and condenses at all cooler parts of the inner cell, including the diamonds. Liquid on the culets can be spotted by the optical microscopes. If the liquid appears the gap is closed to the desired nanometers gap sizes and the scattering experiment starts. X-ray reflectivity is used to determine the out-of-plane structure, such as molecular layering. Horizontal scanning of the detector yields the in-plane structure.

IV. FIRST EXPERIMENTS

First experiments have been carried out at beamline P08 at the synchrotron radiation source PETRA III at DESY in Hamburg, Germany.¹³ As mentioned above the photon energy was set to 18 keV. To concentrate a sufficient number of photons into the gap the beam size was focused to $40 \times 4\ \mu\text{m}^2$ (horizontal times vertical). The divergence was approximately 0.01° (FWHM) in both directions which enables measurement with sufficiently high resolution in q -space. A point detector (Cyberstar NaI scintillation counter, FMB Oxford) and two defining slits have been used to take the data. The first slit was positioned at 400 mm from the sample with an opening of $0.2\ \text{mm} \times 0.2\ \text{mm}$. The second was placed at 1010 mm from the sample with $0.5\ \text{mm} \times 0.5$ aperture, directly in front of the detector. This setup turned out to be only useful for this experiment. The attempt to use a 2D flat panel detector (Perkin Elmer) and a 1D Mythen silicon strip detector (Dectris) had failed as the scattering background from the windows, the benzene gas, and the air had fully dominated the data in the in-plane direction and useful information could not be extracted. The investigated liquid was benzene (Sigma-Aldrich Chromasolv Plus, for high-performance liquid chromatography). After aligning and characterizing the single diamonds by X-ray methods the liquid has been injected in the bottom part of the sample cell which was heated to 27°C at a room temperature of 25°C .

X-ray reflectivity data (see Fig. 6) have been used to determine the thickness of the closed gap. Qualitatively, a closed gap (approximately $< 0.5\ \mu\text{m}$) can be identified by the missing total reflection region which extends from $q_z = 0$ to $q_z = 0.039\ \text{\AA}^{-1}$ for diamond surfaces. Total reflection appears at uncovered surfaces as the refractive index n for X-rays is slightly smaller than 1 with $n = 1 - \delta$ (ignoring the absorption).¹⁴ At closed gaps the X-rays penetrate the diamonds from the side (see Fig. 1) and not from the top. Consequently, no total reflection appears.

At sufficiently small gaps ($< 500\ \text{\AA}$) Kiessig fringes¹⁹ are markers for the gap size. They arise when the reflected X-ray beam from the top and the bottom diamond surfaces interfere. The gap size can be determined from the spacing of these fringes in q_z -space with accuracy better than $1\ \text{\AA}$. At this experiment the gap size was between $200\ \text{\AA}$ and $160\ \text{\AA}$. In a previous experiment with a slightly different setup and with only $200 \times 30\ \mu\text{m}^2$ focus we have achieved gaps down to $50\ \text{\AA}$. The reflectivity curve gives information not only about

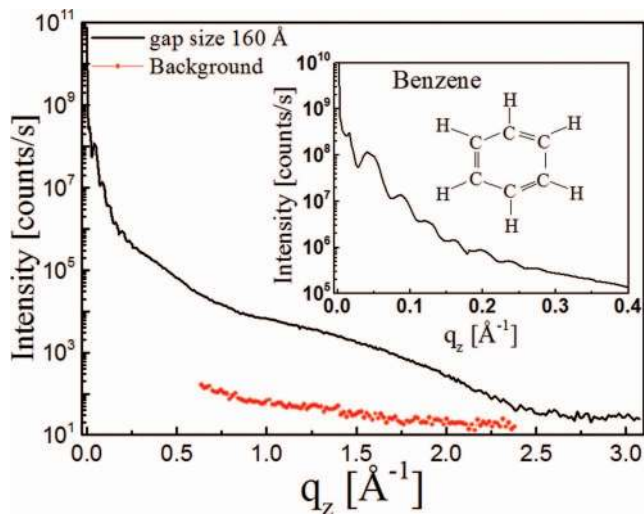


FIG. 6. Reflectivity curve ($\alpha_i = \alpha_f$ during the scan see Fig. 1) of a confined benzene film measured at a gap size of 160 Å. The background has been measured with an offset of 0.1° between incident and exit angles. The inset shows the same data at small q_z .

the spacing. Actually, the detailed electron density profile along the z -direction¹⁴ (see Fig. 1 for the direction of z) can be determined. For this an accurate background subtraction is mandatory. To measure the background scattering we executed an offset scan which is just as a reflectivity scan but with an offset of in our case 0.1° between incident and reflected beam (shown as symbols in Fig. 6). It is obvious that the maximum at approximately 1.5 \AA^{-1} of the reflectivity curve is not dominated by the background. It is most probably on account of layering of the benzene molecules along the z -direction.

Of particular interest is, as mentioned in the Introduction, the in-plane ordering of the liquid molecules which can be detected close to the structure factor peak at $q = 1.4 \text{ \AA}^{-1}$ for benzene bulk. It is extremely challenging to measure the in-plane structure of the confined liquid due to the small amount of liquid. At open surfaces the in-plane scattering cross section can be enhanced significantly by so-called X-ray grazing incidence diffraction methods where evanescent waves evolve on illumination below the critical angle of total reflection.²⁰ However, as explained above total reflection does not occur at the confined liquid samples and amplification of the scattering cross section is not expected. Therefore, it is required to focus as many photons as possible into the gap without losing too much q_z resolution. It turns out that in-plane scattering can be observed with a $40 \times 4 \text{ \mu m}^2$ but not with a $200 \times 30 \text{ \mu m}^2$ focus (not shown) as the small focus concentrates roughly ten times more X-ray photons into the gap as the large beam does. The in-plane scattering achieved with the small focus is displayed in Fig. 7. The curve is already background subtracted where the background has been taken at 6 \mu m vertically shifted gap. Notably, the in-plane scattering of the confined liquid is slightly different from the bulk scattering even though the gap size is larger than ten molecular diameters and the liquid is not in a purely confined state. One issue concerning the data may be the high flux density due to

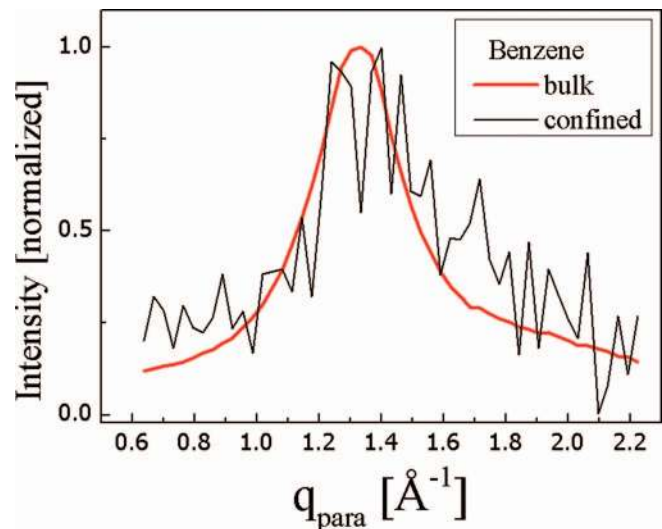


FIG. 7. The in-plane structure factors of the liquid. The noiseless data is from the bulk. The structure factor of the confined liquid is measured at a gap size of 160 Å. The curves are corrected for the background and normalized.

the strong focusing (beam damage), something which has to be investigated in more detail.

V. CONCLUSION

We have designed a setup for X-ray investigations of liquids confined between two plates. The smallest gap size we could achieve is about 50 Å which is of the order of some molecular diameters of the used liquid benzene. The confinement area was roughly $1/8 \text{ mm}^2$. In-plane and out-of-plane X-ray scattering measurements have been carried out. The results are very interesting and could contribute to the understanding of liquids in confinement. Attaining gap sizes on the atomic level requires better quality of the cuvet surfaces and further achievements in the cleaning procedure.

- ¹Y. Xia, G. Dosseh, D. Morineau, and Ch. Alba-Simionesco, *J. Phys. Chem. B* **110**, 19735 (2006).
- ²B. Maier and J. O. Rädler, *Phys. Rev. Lett.* **82**, 1911 (1999).
- ³J. N. Israelachvili, P. M. McGuiggan, and A. M. Homola, *Science* **240**, 189 (1988).
- ⁴J. Klein and E. Kumacheva, *Science* **269**, 816 (1995).
- ⁵O. H. Seeck, H. Kim, D. R. Lee, D. Shu, I. D. Kaendler, J. Basu, and S. K. Sinha, *Europhys. Lett.* **60**, 376 (2002).
- ⁶S. Chodankar, E. Perret, K. Nygård, O. Bunk, D. K. Satapathy, R. M. Espinosa Marzal, T. E. Balmer, M. Heuberger, and J. F. van der Veen, *Europhys. Lett.* **99**, 26001 (2012).
- ⁷R. H. Coridan, N. W. Schmidt, G. H. Lai, P. Abbamonte, and G. C. L. Wong, *Phys. Rev. E* **85**, 031501 (2012).
- ⁸B. Bhushan, J. N. Israelachvili, and U. Landman, *Nature* **374**, 607 (1995).
- ⁹A. Dhinojwala, S. Chul Bae, and S. Granick, *Tribol. Lett.* **9**, 55 (2000).
- ¹⁰M. J. Zwanenburg, J. H. H. Bongaerts, J. F. Peters, D. O. Riese, and J. F. van der Veen, *Phys. Rev. Lett.* **85**, 5154 (2000).
- ¹¹T. Becker, "Collapse Dynamics of confined Liquid Films, PhD Thesis" Ph.D. thesis (University of Twente, 2005).
- ¹²E. Perret, K. Nygard, D. K. Satapathy, T. E. Balmer, O. Bunk, M. Heuberger, and J. F. van der Veen, *J. Phys.: Condens. Matter* **22**, 235102 (2010).

- ¹³O. H. Seeck, C. Deiter, K. Pflaum, F. Bertram, A. Beerlink, J. Horbach, H. Schulte-Schrepping, H. Franz, B. M. Murphy, M. Greve, and O. Magnussen, *J. Synchrotron Radiat.* **19**, 30 (2011).
- ¹⁴J. Als-Nielsen and D. McMorrow, *Elements of Modern X-ray Physics* (Wiley, New York, 2001).
- ¹⁵A. Jayaraman, *Rev. Mod. Phys.* **55**, 65 (1983).
- ¹⁶D. Roundy and M. L. Cohen, *Phys. Rev B* **64**, 212103 (2001).
- ¹⁷M. I. Eremets, *High Pressure Experimental Methods* (Oxford University Press, 1996).
- ¹⁸H. Casimir, Proc. Kon. Nederland. Akad. Wetensch. **B51**, 793 (1948).
- ¹⁹H. Kiessig, *Ann. Phys.* **402**, 769 (1931).
- ²⁰H. Dosch, *Critical Phenomena at Surfaces and Interfaces*, Springer Tracts in Modern Physics Vol. 126 (Springer, Berlin, Heidelberg, 1992).